6. Extract genomic DNA from the frozen samples of 10 consecutive slices, using QIAamp DNA Micro Kit (QIAGEN, Hilden, Germany) or other DNA extraction kits (*see* **Note 3**).

### 2.2 Bisulfite Treatment

1. Freshly prepare the following three solutions (*see* **Note 4**):
   (a) 25 mL of 6 M NaOH by dissolving 6 g of NaOH (pellet) in 24.2 mL of distilled water (DW).
   (b) 5 mL of 4.04 M sodium bisulfite by dissolving 1.92 g of sodium metabisulfite ($Na_2S_2O_5$) in 4.4 mL of DW.
   (c) 10 mL of 10 mM hydroquinone by dissolving 11 mg of hydroquinone in 10 mL of DW.
2. Freshly prepare 120 μL of '3.6 M sodium bisulfite, 0.6 mM HQ (pH 5.00)' solution, by mixing 107 μL of 4.04 M sodium bisulfite, 7 μL of 10 mM hydroquinone, and 6 μL of 6 M NaOH (*see* **Note 5**).
3. Also, prepare the following materials.
   (a) Sonicator for fragmentation of genomic DNA.
   (b) Wizard DNA Clean-Up System (Promega) or other desalting kits.
   (c) 5 M $NH_4OAc$.

### 2.3 MassARRAY

Besides MALDI-TOF mass spectrometry (MassARRAY, Sequenom, San Diego, CA) and the Installation CD, prepare the following materials:

1. 384 microtiter PCR plate for sample reaction.
2. 384 thermocycler.
3. 96-well v-bottom plate for preparation of reaction solution.
4. Bisulfite-treated DNA for template.
5. Hot start Taq polymerase.
6. dNTPs.
7. Primers.
8. Clean Resin.
9. MassCLEAVE Reagent Kit (Sequenom).
   T7 Polymerase (Sequenom).
   T Cleavage Mix (Sequenom).
   C Cleavage Mix (Sequenom).
   SAP (Shrimp Alkaline Phosphatase, Sequenom).
   5× T7 R&DNA Polymerase Buffer (Sequenom).
   RNaseA (Sequenom).
   DTT 100 mM (Sequenom).
   4 Point Calibrant (Sequenom).
10. 384-element SpectroCHIP (Sequenom).

### 2.4 Hierarchical Clustering

1. GeneSpring 7.3.1 software (Agilent technology, Santa Clara, CA) or other software for clustering.

## 3 Methods

### 3.1 Bisulfite Treatment

By bisulfite treatment, cytosine (C) is converted to uracil (U), i.e., thymine (T) after PCR amplification. But methylcytosine (mC) is not converted, i.e., cytosine (C) after PCR amplification.

1. Fragment genomic DNA by sonication.
2. Suspend the 500 ng of fragmented DNA in DW in a volume of 19 μL.
3. Mix the 19 μL of DNA solution with 1 μL of freshly prepared 6 M NaOH (*see* **Note 6**).
4. Incubate at 37 °C for 15 min for denaturation.
5. To the solution, add 120 μL of '3.6 M sodium bisulfite, 0.6 mM HQ' solution, and the solution is subject to 15 cycles of denaturation at 95 °C for 30 s and incubation at 50 °C for 15 min (*see* **Note 7**).
6. Desalt the samples with Wizard DNA Clean-Up System or other desalting kits and elute in 50 μL of TE.
7. To the 50 μL sample solution, add 2.5 μL of 6 M NaOH, and desulfonate by incubation at room temperature for 5 min.
8. Mix with 35 μL of 5 M $NH_4OAc$ and 220 μL of 100 % ethanol, keep at −80 °C for 20 min or overnight, and centrifuge at 15,000 rpm (20,000 × *g*) for 20 min to precipitate DNA. After washing with 70 % ethanol and drying, dissolve in 40 μL of DW.

### 3.2 PCR Amplification

Design bisulfite PCR primers to include no or only one CpG site in a primer sequence, to amplify DNA region containing several CpG sites. PCR product will be 200–500 bp in length. For C at CpG site within a primer sequence, choose a nucleotide which does not anneal to C or U, such as adenosine (A). Primer sequences of Group-1 and Group-2 markers to epigenotype colorectal cancer were previously designed and shown [6]. All the primers were already validated for their quantitativity by calculating correlation coefficient ($R^2$) of standard curve using methylation control samples (0, 25, 50, 75, and 100 % methylation) at each CpG unit. Exclude the CpG units with $R^2 \leq 0.9$ for analysis. Use primer pairs whose amplicon contained 3 or more CpG units with $R^2 > 0.9$ [6].

1. Add 10-mer tag sequence (5′-aggaagagag-) to the 5′ end of the forward primer, and add the T7 promoter sequence and insert sequence (5′-cagtaatacgactcactatagggagaaggct-) to the 5′ end of the reverse primer (Fig. 1). Using these primers, perform PCR amplification as follows.

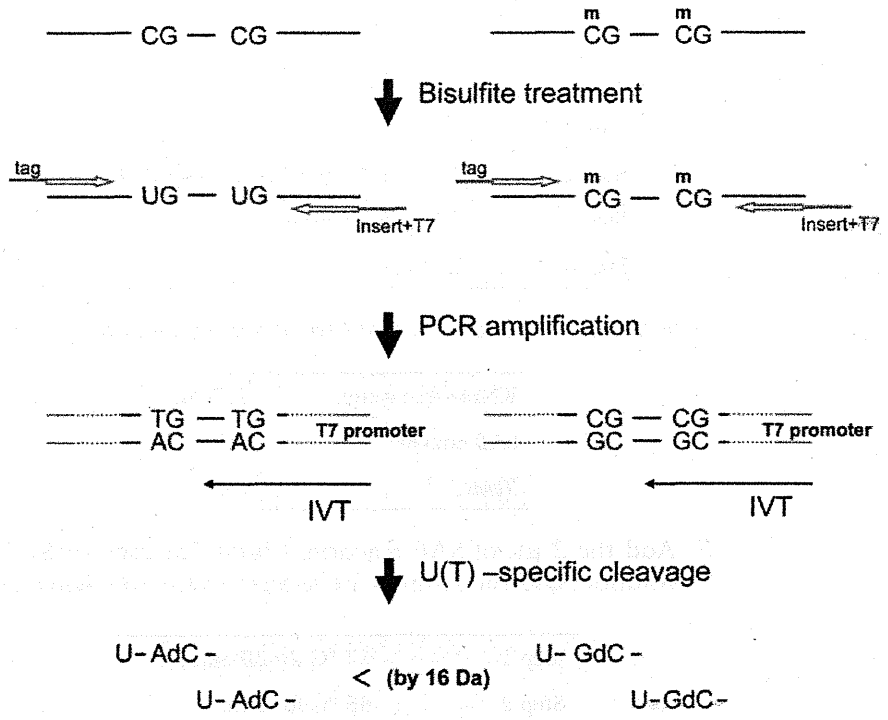


**Fig. 1** Scheme of methylation analysis using MassARRAY. Bisulfite-treated DNA is amplified by PCR, and PCR product is transcribed by in vitro transcription (IVT) and the RNA was cleaved by RNaseA. Unmethylated cytosine (C) was converted to uracil (U) by bisulfite treatment, i.e., thymine (T) in PCR product, and finally adenine (A) in IVT product. Methylated cytosine (mC) was not converted, i.e., cytosine (C) in PCR product, and finally guanine (G) in IVT product. Methylation status was determined by 16-Da mass difference between A and G in a cleaved RNA product. When the product contains 2 or 3 CpG sites, the mass difference will be 32 or 48 Da. Methylation rate was calculated quantitatively for each cleaved product

2. Prepare the PCR reaction solution:

| | |
|---|---|
| Distilled water | 1.42 μL |
| 10× PCR Buffer | 0.50 μL |
| dNTP mix (25 mM each) | 0.04 μL |
| 5 U/μL Hot start Taq | 0.04 μL |
| Primer mix (Forward and Reverse, 1 μM each) | 2.00 μL |
| *Total* | 4.00 μL |

3. Put 4 μL of the solution in each well of 384-well plate.
4. Add 1 μL of bisulfite-treated DNA as a template.
5. The sample is subject to the following reaction.

| | |
|---|---|
| Step 1 | 94 °C for 15 min |
| Step 2 | 94 °C for 20 s |
| Step 3 | 52 °C for 30 s |
| Step 4 | 72 °C for 1 min, Go to Step 2 (45 cycles) |
| Step 5 | 72 °C for 3 min |
| Step 6 | 4 °C forever |

6. For SAP treatment, prepare the reaction solution:

| | |
|---|---|
| RNase-free water | 1.70 μL |
| SAP enzyme | 0.30 μL |
| *Total* | 2.00 μL |

7. Add the 2 μL of SAP reaction solution to each of 5 μL PCR solution, and the samples are subject to the following cycles:

| | |
|---|---|
| Step 1 | 37 °C for 20 min |
| Step 2 | 85 °C for 5 min |
| Step 3 | 4 °C forever (*see* **Note 8**) |

### 3.3 In Vitro Transcription and RNaseA Cleavage

Using the T7 promoter in the reverse primer sequence in PCR product, perform in vitro transcription (IVT) to obtain IVT product of reverse strand. The IVT product is subject to U(T)-specific cleavage using RNaseA (Fig. 2).

1. Prepare the following reaction solution.

| | |
|---|---|
| RNase-free water | 3.15 μL |
| 5× T7 R&DNA Polymerase Buffer | 0.89 μL |
| T Cleavage Mix | 0.24 μL |
| DTT 100 mM | 0.22 μL |
| T7 R/DNA polymerase | 0.44 μL |
| RNase A | 0.06 μL |
| *Total* | 5.00 μL |

2. Put 5 μL of the solution in each well of 384-well plate. Add 2 μL of SAP-treated samples, and the samples are subject to the following cycle.

| | |
|---|---|
| Step 1 | 37 °C for 3 h |
| Step 2 | 4 °C forever |

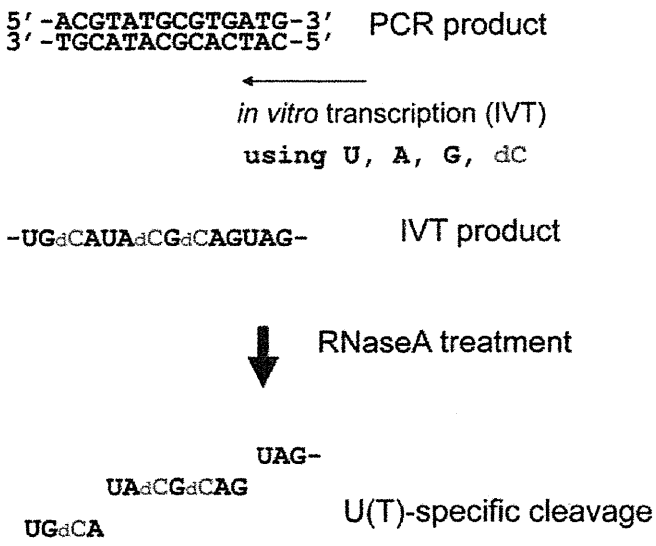


**Fig. 2** U(T)-specific cleavage of IVT product. T Cleavage Mix contains dCTP instead of CTP. Since RNaseA cleaves RNA at the 3′ site of both U(T) and C, and the IVT reaction mixture contains dC instead of C, U(T)-specific cleavage using RNaseA is possible

### *3.4 Purification by Resin and Mass Analysis Using MassARRAY*

Perform quantitative analysis using MassARRAY [6, 17, 18].

1. Add approximately 6 mg of Clean Resin to the sample in each well of 384-well plate.
2. Add 20 μL of RNase-free water in each well, and rotate for 10 min at room temperature.
3. Transfer the resin-purified supernatant to 384-element SpectroCHIP bioarray, then the samples are subject to MALDI-TOF mass spectrometry.

For desorption and ionization of the oligonucleotide, a laser beam irradiates the matrix-oligonucleotide-cocrystal. The ionized product is then accelerated in an electrical field into the TOF device. The TOF device separates the accelerated analyte ions of different mass-to-charge ($m/z$) ratios by providing a field-free drift tube of defined length. After passing the tube, ions are detected and every signal is assigned to a specific molecular mass [19]. Using mass difference of 16 Da between A and G in a cleaved RNA product, mass for unmethylated allele and that for methylated allele is determined, and the ratio is calculated as methylation score (Fig. 3). This analytic unit containing several CpG sites in a cleaved product is called "CpG unit".

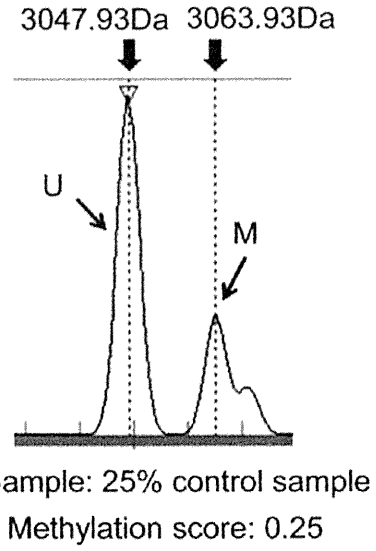


**Fig. 3** Representative MALDI-TOF-MS image of methylation control sample. *X*-axis indicates mass-to-charge ratio (*m/z*) to distinguish 16-Da difference between A and G derived from unmethylated (U) and methylated (M) alleles, respectively. *Y*-axis indicates signal intensity. Using signal intensity, the methylation score is calculated by M/(U+M), which generally gives quantitative results

### 3.5 Mutation Analysis

Mutation at *BRAF* 1799 and *KRAS* 34, 35, and 38 are analyzed by genotyping assay also on MassARRAY platform [19].

1. Design PCR amplification primers and a post-PCR extension primer using MassARRAY Assay Design 3.0 software. The primer sequences are listed in our previous report [12].
2. Perform PCR amplification in a similar manner to the above, in 5 μL volumes containing 0.2 units of Taq polymerase, 5 ng of genomic DNA, 2.5 pmol of PCR primer, and 2.5 nmol of dNTPs. PCR Reactions are cycled at 94 °C for 15 min, followed by 45 cycles of 94 °C for 20 s, 56 °C for 30 s, and 72 °C for 1 min.
3. Perform SAP treatment to deactivate unincorporated dNTPs as above at 37 °C for 20 min and 85 °C for 5 min.
4. Perform post-PCR primer extension using 5.4 pmol of extension primer, 50 μmol of the appropriate dNTP/ddNTP combination, and 0.5 units of Thermosequenase DNA polymerase. Extension reaction are cycled at 94 °C for 30 s, followed by 40 cycles of 94 °C for 5 s, 5 cycles of 52 °C for 5 s and 80 °C for 5 s, and 72 °C for 3 min.
5. Add a cation exchange resin to remove residual salt from the reactions as above.

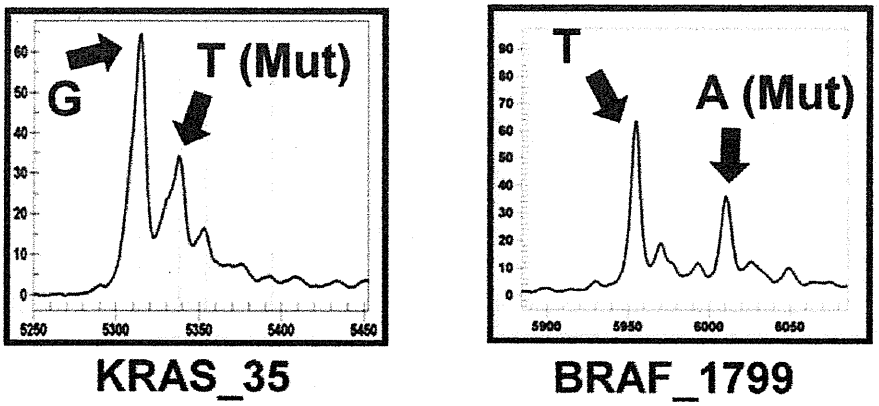


**Fig. 4** Representative MALDI-TOF-MS image of *KRAS*/*BRAF* mutations. *X*-axis indicates mass-to-charge ratio (*m*/*z*) to distinguish wild-type and mutant allele, and *Y*-axis indicates signal intensity

6. Transfer the Resin-purified product to a SpectroCHIP and analyze mass difference using MassARRAY as above. By the difference of molecular mass of nucleotides, the extended base at the possible mutation site is determined (Fig. 4).

### 3.6 Hierarchical Clustering

Unsupervised two-way hierarchical clustering was performed based on Euclid distance correlation and average linkage clustering algorism in sample and marker directions using GeneSpring 7.3.1 or other clustering software packages. The heatmap was drawn using Java TreeView software (http://jtreeview.sourceforge.net/). In the sample direction, CRC cases will be clustered into three groups: high-, intermediate-, and low-methylation epigenotypes. *BRAF*-mutation(+) cases are significantly enriched in high-methylation epigenotype, and *KRAS*-mutation(+) cases are significantly enriched in low-methylation epigenotype. In the marker direction, methylation markers will be clustered into two groups: Group-1 markers with methylation in high-methylation CRC cases, and Group-2 markers with methylation in high- and intermediate-methylation CRC cases (Fig. 5).

## 4 Notes

1. Tumor cells can be enriched by excluding necrotic or inflammatory lesions by macrodissection. Or laser capture microdissection can also be performed.
2. This step is critical for epigenotyping. Samples without enough tumor cells provide uninformative methylation results, which could interfere hierarchical clustering.

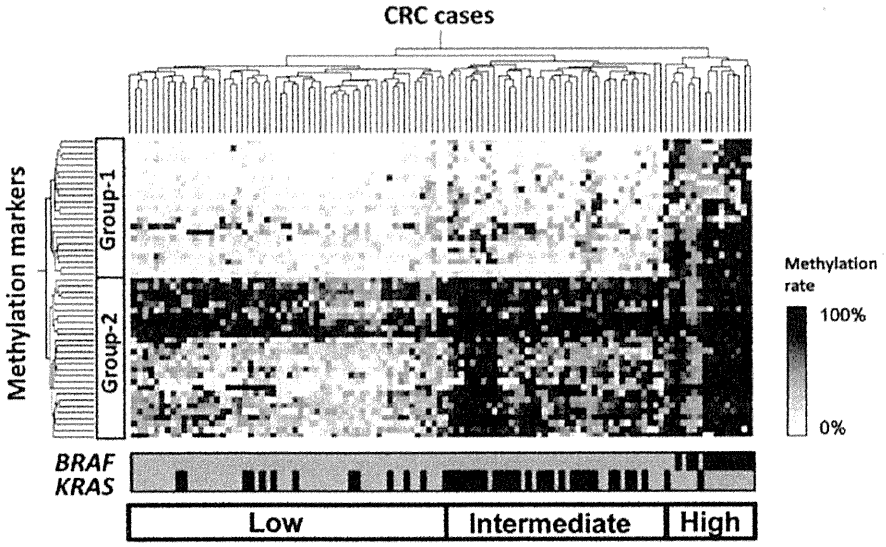


**Fig. 5** Representative result of two-way hierarchical clustering of CRC using quantitative methylation data. CRC cases will be clustered into three epigenotypes, correlating with oncogene mutations

3. More slices can be collected. In that case, the last slice is recommended to be stained with H/E and examined for tumor cell contents.
4. These solutions must be prepared immediately before bisulfite treatment step. Especially, sodium bisulfite solution is very unstable.
5. Bisulfite conversion must be performed at pH 5.0–5.2. If the "3.6 M sodium bisulfite, 0.6 mM HQ" solution is prepared as shown, the pH will be 5.00, and be increased to 5.0–5.2 when mixed with denatured DNA solution at the **step 5** of Subheading 3.1.
6. It is more accurate to add 5 μL of 1.2 M NaOH to 15 μL of 500 ng DNA solution.
7. Due to the NaOH in the denaturation, the pH of the solution will increase to ~5.1.
8. It is recommended to check PCR product by electrophoresis of 1.5 μL of the solution using 2 % agarose gel.

## Acknowledgement

This work was supported by a grant of Core Research for Evolutionary Science and Technology (CREST), Japan Science and Technology Agency, and Grants-in-Aids for Scientific Research from Ministry of Education, Culture, Sports, Science, and Technology of Japan.

## References


1. Feinberg AP, Tycko B (2004) The history of cancer epigenetics. Nat Rev Cancer 4: 143–153
2. Esteller M (2008) Epigenetics in cancer. N Engl J Med 358:1148–1159
3. Jones PA, Baylin SB (2007) The epigenomics of cancer. Cell 128:683–692
4. Grady WM, Carethers JM (2008) Genomic and epigenetic instability in colorectal cancer pathogenesis. Gastroenterology 135:1079–1099
5. Shen L, Toyota M, Kondo Y, Lin E, Zhang L, Guo Y et al (2007) Integrated genetic and epigenetic analysis identifies three different subclasses of colon cancer. Proc Natl Acad Sci U S A 104:18654–18659
6. Yagi K, Akagi K, Hayashi H, Nagae G, Tsuji S, Isagawa T et al (2010) Three DNA methylation epigenotypes in human colorectal cancer. Clin Cancer Res 16:21–33
7. Hinoue T, Weisenberger DJ, Lange CP, Shen H, Byun HM, Van Den Berg D et al (2012) Genome-scale analysis of aberrant DNA methylation in colorectal cancer. Genome Res 22: 271–282
8. Vogelstein B, Fearon ER, Hamilton SR, Kern SE, Preisinger AC, Leppert M et al (1988) Genetic alterations during colorectal-tumor development. N Engl J Med 319:525–532
9. Feinberg AP, Ohlsson R, Henikoff S (2006) The epigenetic progenitor origin of human cancer. Nat Rev Genet 7:21–33
10. Toyota M, Ahuja N, Ohe-Toyota M, Herman JG, Baylin SB, Issa JP (1999) CpG island methylator phenotype in colorectal cancer. Proc Natl Acad Sci U S A 96: 8681–8686
11. Weisenberger DJ, Siegmund KD, Campan M, Young J, Long TI, Faasse MA et al (2006) CpG island methylator phenotype underlies sporadic microsatellite instability and is tightly associated with BRAF mutation in colorectal cancer. Nat Genet 38:787–793
12. Yagi K, Takahashi H, Akagi K, Matsusaka K, Seto Y, Aburatani H et al (2012) Intermediate methylation epigenotype and its correlation to KRAS mutation in conventional colorectal adenoma. Am J Pathol 180:616–625
13. Kim YH, Kakar S, Cun L, Deng G, Kim YS (2008) Distinct CpG island methylation profiles and BRAF mutation status in serrated and adenomatous colorectal polyps. Int J Cancer 123:2587–2593
14. Snover DC (2011) Update on the serrated pathway to colorectal carcinoma. Hum Pathol 42:1–10
15. Kaneda A, Yagi K (2011) Two groups of DNA methylation markers to classify colorectal cancer into three epigenotypes. Cancer Sci 102:18–24
16. Nosho K, Irahara N, Shima K, Kure S, Kirkner GJ, Schernhammer ES et al (2008) Comprehensive biostatistical analysis of CpG island methylator phenotype in colorectal cancer using a large population-based sample. PLoS One 3:e3698
17. Ehrich M, Nelson MR, Stanssens P, Zabeau M, Liloglou T, Xinarianos G et al (2005) Quantitative high-throughput analysis of DNA methylation patterns by base-specific cleavage and mass spectrometry. Proc Natl Acad Sci U S A 102:15785–15790
18. Coolen MW, Statham AL, Gardiner-Garden M, Clark SJ (2007) Genomic profiling of CpG methylation and allelic specificity using quantitative high-throughput mass spectrometry: critical evaluation and improvements. Nucleic Acids Res 35:e119
19. Vogel N, Schiebel K, Humeny A (2009) Technologies in the Whole-Genome Age: MALDI-TOF-Based Genotyping. Transfus Med Hemother 36:253–262

# NR4A3, a possibile oncogenic factor for neuroblastoma associated with CpGi methylation within the third exon

SHOTA UEKUSA[1,2*], HIROYUKI KAWASHIMA[1,2*], KIMINOBU SUGITO[1], SHINSUKE YOSHIZAWA[1,2], YUI SHINOJIMA[2], JUN IGARASHI[2,3], SRIMOYEE GHOSH[4], XAOFEI WANG[2,3,5], KYOKO FUJIWARA[2,6,7], TARO IKEDA[1], TSUGUMICHI KOSHINAGA[1], MASAYOSHI SOMA[6,7] and HIROKI NAGASE[2,3,5,7]

Departments of [1]Pediatric Surgery and [2]Cancer Genetics, School of Medicine, [3]Life Science Advanced Research Institute for the Sciences and Humanities, Nihon University, Tokyo, Japan; [4]Department of Zoology, North-Eastern Hill University, Meghalaya, India; [5]Chiba Cancer Center Research Institute, Chiba; [6]Innovative Therapy Research Group, Nihon University Research Institute of Medical Science, [7]Division of General Medicine, Department of Medicine, Nihon University School of Medicine, Tokyo, Japan

Received December 18, 2013; Accepted February 12, 2014

DOI: 10.3892/ijo.2014.2340

**Abstract.** Aberrant methylation of *Nr4a3* exon 3 CpG island (CpGi) was initially identified during multistep mouse skin carcinogenesis. *Nr4a3* is also known as a critical gene for neuronal development. Thus, we examined the *Nr4a3* exon 3 CpGi methylation in mouse brain tissues from 15-day embryos, newborns and 12-week-old adults and found significant increase of its methylation and Nr4a3 expression during mouse brain development after birth. In addition, homologous region in human genome was frequently and aberrantly methylated in neuroblastoma specimens. A quantitative analysis of DNA methylation revealed that hypomethylation of CpG islands on *NR4A3* exon 3, but not on exon 1 was identified in three neuroblastomas compared with matched adrenal glands. Additional analysis for 20 neuroblastoma patients was performed and 8 of 20 showed hypomethylation of the CpGi on *NR4A3* exon 3. The survival rate of those 8 patients was significantly lower compared with those in patients with hypermethylation. Immunohistochemical NR4A3 expression was generally faint in neuroblastoma tissues compared with normal tissues. Moreover, the MYCN amplified NB9 cell line showed hypomethylation and low expression of *NR4A3*, while the non-MYCN amplified NB69 cell line showed hypermethylation and high expression. These results indicate that DNA hypomethylation of the CpGi at *NR4A3* exon 3 is associated with low *NR4A3* expression, and correlates with poor prognosis of neuroblastoma. Since NR4A3 upregulation associated with the hypermethylation and neuronal differentiation in mice, poor prognosis of neuroblastoma associated with NR4A3 low expression may be partly explained by dysregulation of its differentiation.

*Correspondence to:* Professor Hiroki Nagase, Chiba Cancer Center Research Institute, 666-2 Nitona-Cho, Chuo-Ku, Chiba 260-8717, Japan
E-mail: hnagase@chiba-cc.jp

*Contributed equally

*Abbreviations:* T-DMRs, tissue-specific differentially methylated regions; DS-DMRs, developmental stage differentially methylated regions; CpGi, CpG island; E15, 15-day-old embryo; NB, new born; AD, 12-week adult; TrkA, tropomyosin receptor kinase A; NGF, nerve growth factor; hMC, homogeneous MassCLEAVE; MALDI-TOF MS, matrix-assisted laser desorption/ionization time-of-flight mass spectrometry; Tm, melting temperature; PCR, polymerase chain reaction; TBS, Tris-buffered saline; PBS, phosphate-buffered saline; CTCF, CCCTC binding factor; UTR, untranslated region; AUF1, AU-rich element binding factor 1; HUR, Hu antigen R

*Key words:* nuclear receptor subfamily 4, group A, member 3, DNA methylation, neuroblastoma

## Introduction

Neuroblastoma is an embryonic tumor of neuroectodermal cells derived from the neural crest. It is the most common extracranial solid tumor in children, and it accounts for approximately 15% of all pediatric oncology death. Survival rate of the patient with high-risk neuroblastoma is still <40%, despite combined modality therapy (1,2).

Recent advances have disclosed the significance of epigenetic events in the development and progression of human tumorigenesis. Generally, global DNA methylation levels are low in cancer and has been linked to genomic instability, which can lead to DNA damage. On the other hand, promoter-specific hypermethylation of specific genes, such as tumor suppressor genes, is the most common event in tumorigenesis (3). It is also reported that predetermined epigenetic program provides required direction for the number of changes during embryonic and postnatal development that are necessary for proceeding from an oocyte to a fully developed adult animal (4). DNA methylation is the one of the best-characterized epigenetic modifications and plays an important role in the diverse genomic processes,

Table I. The tissue samples analyzed.

| Patient | Age at diagnosis (month) | INSS | INPC | Shimada classification | Copy nos. of *MYCN* | Prognosis (month) | Methylation level of *NR4A3* exon 3 (%)[a] |
|---|---|---|---|---|---|---|---|
| Case 1 | 6 | 1 | NBL, D | FH | 1 | 48S | 43.1±5.9 |
| Case 2 | 10 | 2 | NBL, PD | FH | 1 | 26S | 67.1±2.5 |
| Case 3 | 6 | 2 | NBL, PD | FH | 1 | 48S | 20.1±0.9 |
| Case 4 | 6 | 4S | NBL, UD | FH | 1 | 48S | 43.1±5.9 |
| Case 5 | 6 | 2 | NBL, PD | FH | 1 | 48S | 7.6±0.1 |
| Case 6 | 7 | 2 | NBL, PD | FH | 1 | 48S | 18.4±1.6 |
| Case 7 | 8 | 2 | NBL, PD | FH | 1 | 48S | 83.2±0.4 |
| Case 8 | 26 | 4 | NBL, PD | UH | 10 | 6R | 36.1±1.5 |
| Case 9 | 36 | 4 | NBL, UD | UH | 20 | 48S | -0.4±8.9 |
| Case 10 | 30 | 4 | NBL, PD | UH | 1 | 48S | 34.3±2.4 |
| Case 11 | 47 | 4 | NBL, UD | UH | 20 | 4R | 8.5±1.5 |
| Case 12 | 21 | 3 | NBL, UD | UH | 150 | 7R | 2.1±7.3 |
| Case 13 | 98 | 3 | NBL, UD | UH | 1 | 48S | -1.2±7.3 |
| Case 14 | 77 | 4 | NBL, PD | UH | 3 | 4S | 14.7±5.9 |
| Case 15 | 79 | 4 | NBL, PD | UH | 3 | 35R | 39.1±2.2 |
| Case 16 | 53 | 4 | NBL, UD | UH | 4 | 24R | 79.4±0.6 |
| Case 17 | 20 | 4 | NBL, UD | UH | 81 | 5R | 9.1±3.8 |
| Case 18 | 68 | 4 | NBL, PD | UH | 1 | 10R | 5.2±2.5 |
| Case 19 | 18 | 4 | NBL, PD | UH | 119 | 37S | 5.4±4.1 |
| Case 20 | 33 | 4 | NBL, UD | UH | 1 | 36S | 25.6±10.1 |

INSS, International Neuroblastoma Staging System; INPC, International Neuroblastoma Pathology Committee; NBL, neuroblastoma; PD, poorly differentiated; UD, undifferentiated; FH, favorable histology; UH, unfavorable histology; S, recurrent free survival; R, recurrent. [a]Data are shown as mean ± SD.

such as gene regulation, chromosomal stability, parental imprinting and X-inactivation (5). Recent genome-wide DNA methylation searches indicate that 4 to 17% of CpG sites are different in methylation among tissues and developmental processes (6-8). The methylation status at the tissue-specific differentially methylated regions (T-DMRs) and developmental-specific differentially methylated regions (DS-DMRs) are suggested to play important roles in development and differentiation.

Nuclear receptor subfamily 4, group A, member 3 (*Nr4a3*), also known as neuron-derived orphan receptor 1 (NOR1), is a member of NR4A subgroup of orphan nuclear receptor. In mammals, the NR4A subgroup consists of NR4A1 (Nur77), NR4A2 (Nurr1) and NR4A3 (9). The monomer form of those receptors binds to the nerve growth factor-induced clone B response element (NBRE), and homodimer or heterodimer forms bind to the Nurl response element in the promoter of their target genes which may be essential for the development of dopaminergic neurons in the midbrain (10). We identified the CpG sites in *Nr4a3* exon 3 as a mouse skin cancer T-DMR and a mouse brain DS-DMR by using analyses of restriction landmark genomic scanning (RLGS) and methyl-DNA immunoprecipitation (MeDIP), respectively (Fujiwara *et al*, unpublished data). Here, we analyzed involvement of DNA methylation at *Nr4a3* exon 3 CpGi in Nr4a3 expression, mouse brain development, neuroblastomagenesis and association with its poor prognosis.

## Materials and methods

*Tissue samples.* C57 BL/6J mice were purchased from Jackson Laboratory (Bar Harbor, ME) and maintained in Oriental Yeast Co. Ltd (Tokyo, Japan). Brain specimens from mice at three different developmental stages: E15, 15-day-old embryo; NB, new born; and AD, 12-week adult; were disected and stored as described previously (11).

Twenty primary neuroblastoma tumors were obtained in Nihon University Hospital (Tokyo, Japan) at the time of diagnosis, from 1999 to 2007. All the analyses of those specimens were performed under the approval of Nihon University Institutional Review Boards (IRB no. 51). Neither neoadjuvant chemotherapy nor irradiation therapy was given preoperatively to any patient. Four adrenal samples were collected from a nephroblastoma patient undergoing nephrectomy and from 3 neuroblastoma patients (cases 3, 8 and 20) undergoing tumor resection. All of the samples were immediately snap-frozen in liquid nitrogen and stored at -80˚C until use. Summary of these patients is shown in Table I.

*Cell lines and culture condition.* Human neuroblastoma cell lines NB9 and NB69 were obtained from Riken Cell Bank (Tsukuba, Japan). Both human neuroblastoma cell lines were maintained in RPMI-1640 (Nalarai Tesque, Kyoto, Japan) supplemented with 15% fetal bovine serum (Nichirei Biosciences, Tokyo, Japan), 100 IU/ml penicillin (Gibco™,

Table II. The primers for quantitative DNA methylation analysis.

| Primer name | | Sequence |
|---|---|---|
| NR3A3-a | Forward | GGAAATTGTTAAGTGTTTTTTTATAT |
| | Reverse 1 | CAACCACCACTTCCTAAAT |
| | Reverse 2 | CGACCACCACTTCCTAAAT |
| NR3A3-b | Forward | AGTTTTAGAATTTATGTAAGAGGAAAG |
| | Reverse 1 | CACCCAACTATCAAACTC |
| | Reverse 2 | CGCCCAACTATCAAACTC |
| NR3A3-c | Forward | GAGGTGTTGTTTAGTATTTTTATGTATTTTAAGTAG |
| | Reverse | CTCACCTTAAAAAAACCCTTACAACC |

Each reverse primer has a T7-promotor tag (5'-cagtaatacgactcactatagggagaaggct-3') for *in vitro* transcription and the forward primer is tagged with a 10 mer tag (5'-aggaagagag-3') to balance Tm.

Carlsbad, CA) and 100 µl/ml streptomycin (Gibco). The cells were cultured in a 37°C humidified atmosphere containing 5% $CO_2$ maintained in appropriate conditions recommended by the manufacturers.

*DNA preparation and bisulfite treatment.* Total genomic DNA was extracted from mouse brains, primary tumors, neuroblastoma cell lines and normal adrenal medullas with DNeasy Tissue Kit (Qiagen, Valencia, CA) and modified by sodium bisulfite using the EZ DNA Methylation Kit (Zymo Research, Orange, CA), by following the manufacturer's instructions.

*Quantitative analysis of DNA methylation using base-specific cleavage and matrix-assisted laser desorption/ionization time-of-flight mass spectrometry (MALDI-TOF MS).* Sequenom MassARRAY quantitative methylation analysis (12) using the MassARRAY Compact System (www.sequenom.com) was employed for the quantitative DNA methylation analysis at CpG dinucleotides. This system utilizes mass spectrometry (MS) for the detection and quantitative analysis of DNA methylation using homogeneous MassCLEAVE (hMC) base-specific cleavage and matrix-assisted laser desorption/ionization time-of-flight (MALDI-TOF) MS (13). The MethPrimer program (http://www.urogene.org/methprimer/index1.html) (12) was used to design bisulfite PCR primers (Table II). Each reverse primer has a T7-promotor tag for *in vitro* transcription (5'-cagtaatacgactcactatagggagaaggct-3'), and the forward primer is tagged with a 10 mer to balance melting temperature (TM) (5'-aggaagagag-3'). All primers were purchased from Operon (Tokyo, Japan). Polymerase chain reaction (PCR) amplification was performed using HotStarTaq Polymerase (Qiagen) in a 5 µl reaction volume using PCR primers at a 200 nM final concentration, and bisulfate treated DNA (~20 ng/ml). After the treatment of shrimp alkaline phosphatase, 2 µl of the PCR products was used as a template for *in vitro* transcription and RNase A Cleavage for the T-reverse reaction (3' to either rUTP or rCTP), as described in the manufacturer's instructions (Sequenom hMC, Sequenom, San Diego, CA). The samples were desalted and spotted on a 384-pad SpectroCHIP (Sequenom) using a MassARRAY nanodispenser (Samsung Seoul, Korea), followed by spectral acquisition on a MassARRAY Analyzer Compact MALDI-TOF MS (Sequenom). The resultant methylation calls were analyzed by EpiTYPER software v1.0 (Sequenom) to generate quantitative measurements for each CpG site or an aggregate of multiple CpG sites. Since maldi-TOF mass methylated peaks do not denote a particular CpG site, but rather corresponds to the number of CpG sites methylated within the cleavage fragment, we decided to present average percent methylation of all CpG sites in the bisulfite PCR fragment with the standard curve.

Standard curve of DNA methylation level was made by using 0, 25, 50, 75 and 100% methylated samples. BAC DNA (RPMI-11 341L6) obtained from Roswell Park Cancer Institute (Buffalo, NY) was used as 0% methylation and M.Sss-1 double treated BAC DNA was used as 100% methylation. The PCR was carried out with a final volume of 50 µl, containing 1.0 µl of each 10.0 µM primer (final concentration 0.2 µM), 8.0 µl of 2.5 mM dNTP, 25 µl of 2 times GC Buffer (Takara Bio, Shiga, Japan), 0.5 U of LA taq (Takara Bio) and 1 µl of genomic DNA as a template. Amplification was carried out with an initial denaturing at 94°C for 1 min followed by 45 cycles of denaturing at 94°C for 30 sec, annealing for 1 min at the annealing temperature of each primer (60°C), extension for 3 min at 72°C, and then a final extension for 5 min at 72°C. The methylation reactions were carried out in 1X M.SssI buffer with 160 µM SAM (New England Biolabs, Ipswich, MA). In total reaction volume of 50 µl, 500 ng PCR product was treated with 4U M.SssI for 1 h at 37°C. Reactions were stopped for 20 min at 65°C and PCR product was purified Qiagen PCR purification kit (Qiagen). This CpG methyltransferase reaction was performed twice. Then M.SssI treated PCR product was produced (14). Curve was fitted and methylation levels were modified.

*Western blot analysis.* All of samples were collected and total cell lysates were prepared in M-PER mammalian protein extraction reagent (Thermo, Rockford, IL) containing a protease-inhibitor cocktail (Nalarai Tesque). Proteins (20 µg) were loaded on NuPAGE + 10% Bis-Tris gels (Invitrogen Life Technologies, Carlsbad, CA) for electrophoresis. The proteins were separated at 100 mA for 1 h, then transferred to polyvinylidene difluoride membranes by using iblot transfer

for 7 min (Invitrogen). The membranes were incubated with Tris-buffered saline (TBS), containing 5% non-fat milk, 0.2% Tween-20 and a rabbit anti-NR4A3 polyclonal antibody (1:100) overnight (SC-30154, Santa Cruz Biotechnology, Santa Cruz, CA). The membranes were washed three times with a TBS containing 0.2% Tween-20. The immunocomplexed proteins were identified by reaction with a peroxidase-linked goat antibody to rabbit IgG (GE Healthcare, Little Chalfont, UK). Then these immunocomplexed proteins were detected by enhanced chemiluminescent reaction (Amersham Bioscience Inc., Piscataway, NJ). Immunoblotting with antibody to actin (Abcam, Cambridge, MA) provided an internal control for equal protein loading. Chemiluminescent detection was performed by LAS4000 (Fujifilm, Tokyo, Japan).

*Immunohistochemical staining.* Formalin-fixed, paraffin-embedded serial sections (4 $\mu$m) were deparaffinized in xylene, rehydrated through graded alcohols, and immersed for 15 min in phosphate-buffered saline (PBS). The sections were soaked in 10 mmol/l of sodium citrate buffer (pH 6.9) and treated in a microwave for 15 min for antigen retrieval. After antigen retrieval the endogenous peroxidase activity was blocked with 3% hydrogen peroxidase in methanol for 30 min, and non-specific staining was then blocked by 1-h incubation with normal goat serum (Nichirei Biosciences). The sections were then incubated overnight at 4°C with 2 $\mu$g/ml of a rabbit anti-NR4A3 polyclonal antibody (SC-30154: Santa Cruz Biotechnology). The sections were treated for 30 min at room temperature with goat secondary antibody against rabbit immunoglobulins (Nichirei Biosciences). The sections were stained at room temperature for 25 min with AEC substrate kit (Vector Laboratories, Burlingame, CA). After staining with AEC substrate kit the sections were counterstained with hematoxylin.

*Chromatin immunoprecipitation assays.* Chromatin immunoprecipitation assays were performed essentially as previously described (15-17) with the following minor modifications. Neuroblastoma cell lines (NB9 and NB69) were fixed in 0.33 M (1%) formaldehyde for 10 min, before adding 4 volumes of ice-cold PBS containing 0.125 M glycine, to give an approximately 2-fold molar excess of glycine over formaldehyde. Then cells were washed with cold PBS containing Protease K (Nalarai Tesque). Crude cell lysates were sonicated to generate 200-1,000 bp DNA fragments. Chromatin was immunoprecipitated with 10 $\mu$l of rabbit antiserum raised against human CTCF (07-729; Millipore, Billerica, MA) per $1x10^7$ cells or with 2 $\mu$g normal rabbit immunoglobulin G (IgG; Millipore) used as a control, according to manufacturer's protocols (Millipore). PCR amplification was performed using AccuPrime (Invitrogen) in a 25 $\mu$l reaction volume using PCR primers at 200 nM final concentration and 5 $\mu$l immunoprecipitated DNA as a template. Amplification was carried out with an initial denaturing at 94°C for 1 min followed by 38 cycles of denaturing at 94°C for 30 sec, annealing for 30 sec at the annealing temperature of each primer, extension for 1 min at 68°C, and then a final extension for 5 min at 72°C, using specific primers as follows: for *NR4A3* exon 3, 5'-CTTCCCGCTCTTCCACTTC-3'; and 5'-TCACCTTGAAAAAGCCCTTG-3', Tm 58°C; for cMYC, 5'-GTTTTAAGGAACCGCCTGTCCTTC-3' and 5'-GGATTGCAAATTACTCCTGCCTCC-3', Tm 62°C (18). All primers were purchased from Operon.

*Statistical analysis.* The Mann-Whitney U test was used to evaluate the statistical significance of the difference in the methylation level of *NR4A3* among the samples. The methylation levels were categorized by Youden index using 17 patients passed the observation period (19). The cutoff point between high and low levels of DNA methylation at each DMR was calculated by ROC curve analysis. Survival curves were calculated according to Kaplan-Meier analysis and compared with a log-rank test. Event-free survival was calculated as the time from diagnosis to event or last examination if the patient had no event. Recurrence, progression of disease and death from disease were counted as events. Death resulting from therapy complications or from second malignancy was not counted as an event but censored for event-free survival. The data were analyzed by the SPSS (Chicago, IL) for Windows. Differences were considered significant at $p<0.05$.

## Results

*Methylation levels at CpG sites of Nr4a3 exon 3 CpGi and its expression in mouse brain specimens.* Methylation levels of each CpG site at the *Nr4a3* exon 3 CpG island in mouse brains were analyzed at three different developmental stages. This CpGi (mouse chr4:48072571-48072905 in the USCS database, February, 2006 assembly) showed higher methylation level in the brain specimens of 12-weeks-old mice (AD brain), compared with brain specimens from 15-days-old embryos (E15) or new-born mice (NB) in the analysis using Mass ARRAY EpiTYPER (Fig. 1A). The average methylation level of all CpG sites in this region was significantly higher in AD brain than in E15 and NB brain specimens (Fig. 1B). Western blot analysis revealed higher expression level of NR4A3 protein in AD brain specimens, compared with the other developmental stages (Fig. 1C).

*Search for the most different somatic change within homologous Nr4a3 exon 3 CpGi in human neuroblastoma.* We analyzed methylation level of human homologous region (chr4:48072371-48072905, in USCS genome database, March, 2006, NCBI36/hg18) in the surgical resected NB specimens and found that all 3 NB specimens showed significantly lower methylation level at *NR4A3* exon 3 CpGi compare to those from the matched adrenal tissues (Fig. 2). The CpGi located between *NR4A3* promoter and intron 1 was not methylated at all in either neuroblastoma or adrenal samples.

*Aberrant methylation at NR4A3 exon 3 CpGi confirmed by using Mass ARRAY EpiTYPER method in additional 17 neuroblastoma specimens.* Additional 17 neuroblastoma samples and 1 adrenal sample were used to confirm aberrant methylation at *NR4A3* exon 3 CpGi. Adding a new adrenal sample, all the 4 adrenal samples were hypermethylated at *NR4A3* exon 3 CpGi. The average methylation level in 4 adrenal samples was 64.6±2.1%. The methylation level of neuroblastoma specimens varied from *83.3±.. to *-0.5±0.9%, and the average value of the all samples was 27.0±25.8%, which was significantly lower than the average methylation level of 4 normal samples

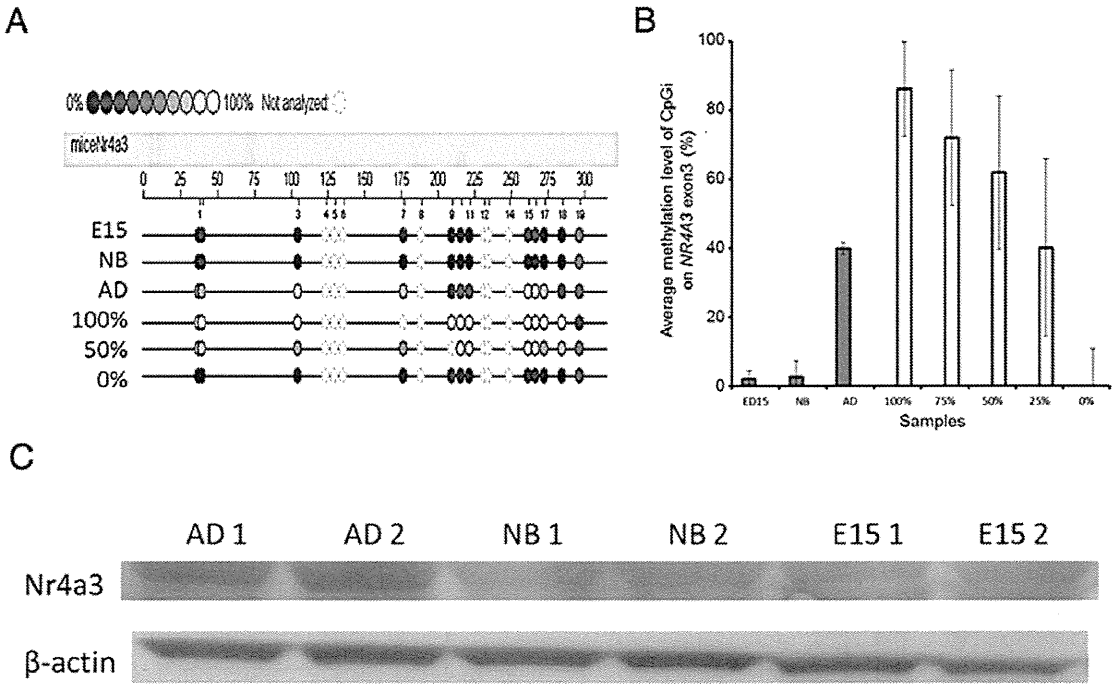


Figure 1. DNA methylation and protein expression levels of NR4A3 in mouse brain samples. DNA methylation level was analyzed quantitatively using Sequenom MassARRAY EpiTYPER. Methylation level is shown in Epigram (A) and average methylation levels are shown in the bar graph (B). Gray columns indicate mouse brain samples and open columns are the standard. Error bars indicate SD. Methylation levels in AD mouse brain samples were significantly higher than those in NB and E15 brains. ($p<0.030$). (C) NR4A3 and loading control of β-actin protein expression was analyzed by western blotting. AD brain showed higher expression level of NR4A3 than in NB and E15.

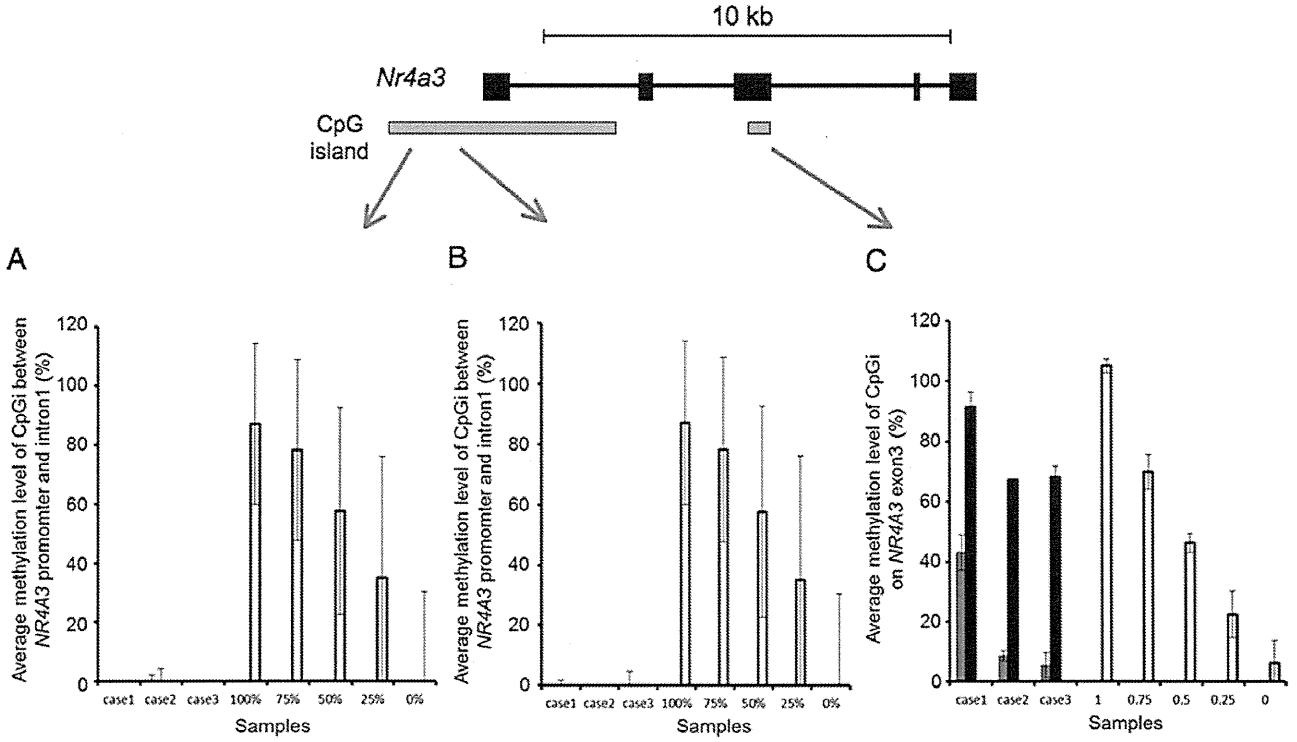


Figure 2. DNA methylation levels of the *NR4A3* region in human neuroblastoma specimens. Methylation levels of human homologous region of *Nr4a3* were analyzed quantitatively using Sequenom MassARRAY EpiTYPER in human neuroblastoma. Methylation levels of CpGi at NR4A3 exon 3 (C), but not in 5' promoter CpGi (A and B), were significantly higher in neuroblastoma than those in corresponding adrenal glands ($p<0.01$). Gray columns indicate neuroblastoma samples, black columns are for adrenal samples and open columns are the standard. Data are shown as mean ± SD.

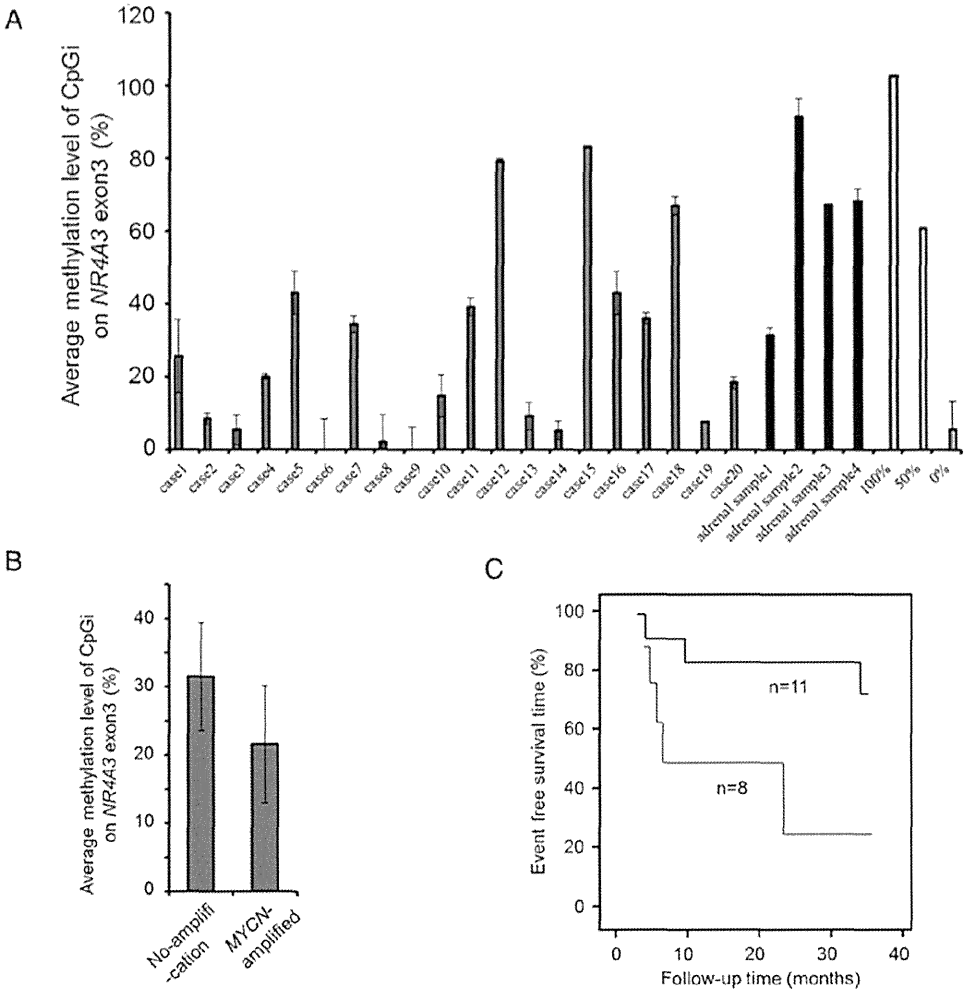


Figure 3. DNA methylation levels of *NR4A3* exon 3 CpGi in additional human neuroblastoma specimens and survival analyses of neuroblastoma patients. Methylation levels in *NR4A3* exon 3 CpGi were analyzed by using Mass ARRAY EpiTYPER method in 20 neuroblastoma specimens and 4 adrenal samples. (A) The bar graphs show the average of methylation levels in the region. Gray columns indicate neuroblastoma samples, black columns are for adrenal samples and open columns are the standard. The error bars indicate SD. (B) Average methylation level of CpGi at NR4A3 exon 3 in 11 samples without MYCN amplification and 9 samples with MCYN amplification are shown. The error bar indicate SEM. (C) Kaplan-Meier analysis was performed to see whether methylation level at NR4A3 exon 3 CpGi associate with the survival length of neuroblastoma patients. Twenty neuroblastoma specimens were segregated into two groups depending on their methylation levels of the *NR4A3* exon 3 regions (hypermethylation, methylation level is higher than 11.93%; hypomethylation, methylation level is 11.93% or lower). Eight out of 20 neuroblastoma specimens were in the hypomethylation tumor group. Black line indicates the hypermethylation group and gray line is for the hypomethylation group. There was a significant association between methylation levels and patient outcome (p=0.034, log-rank test).

(p=0.005, Mann-Whitney U test) (Table I, Fig. 3A). In 17 out of 20 neuroblastoma specimens, methylation levels at *NR4A3* exon 3 CpGi were low, compared with the average methylation level in 4 adrenal samples. Methylation level in 9 *MYCN* amplified neuroblastoma specimens was significantly lower, compared with that in 11 specimens without *MYCN* amplification (Fig. 3B) (p=0.005, Mann-Whitney U test).

For Kaplan-Meier analysis, cut off value of the methylation level was calculated as 11.93% by using youden index and the methylation levels of 20 patients passed the observation period. Twenty neuroblastoma patients were divided into two groups depending on their methylation levels at the *NR4A3* exon 3 regions. The hypermethylation group has methylation level higher than the cut off value, and the hypomethylation group showed lower than that. Eight out of 20 neuroblastoma specimens were classified to hypomethylation group. There was significant association between the methylation level at NR4A3 exon 3 CpGi and patient outcome (p=0.034, log-rank test) (Fig. 3C).

*Immunohistochemical staining (IHC).* Immunohistochemical analysis using NR4A3 antibody showed a strong signal in adrenal tissue sections and pronounced cytoplasmic staining. On the other hand, faint staining was seen in neuroblastoma specimens (Fig. 4).

*Correlation between NR4A3 exon 3 CpGi methylation and NR4A3 protein expression in neuroblastoma cells.* The average methylation level at *NR4A3* exon 3 CpGi in NB9 cells was 44±23.2%, on the other hand, it was 97.1±5.8% in NB69

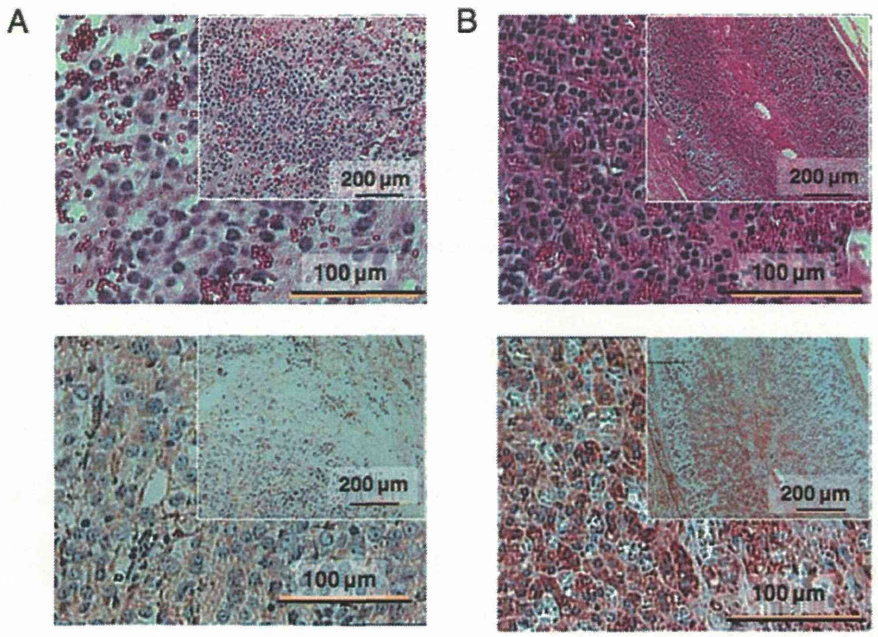


Figure 4. Imunohistochemical analyses of NR4A3 in neuroblastoma and adrenal samples. H&E staining (upper) and immunohistochemical analysis using anti-NR4A3 antibody (lower) were performed for (A) a neuroblastoma section and (B) an adrenal section. Immune reactivity was stronger in adrenal sample than in the neuroblastoma section.

cell (Fig. 5A and B). Western blot analysis revealed higher expression level of NR4A3 protein in NB69 compared with NB9 (Fig. 5C). This result also indicates that NR4A3 protein expression was correlated with *NR4A3* exon 3 CpGi methylation in human neuroblastoma cell lines.

*Chromatin immunoprecipitation assays.* We examined chromatin immunoprecipitation assays to elucidate the mechanism in which methylation level of NR4A3 exon 3 CpGi regulates the expression level. DNA purified from the immunoprecipitated chromatin using anti-CTCF antibody was amplified by PCR for a candidate CTCF binding site of NR4A3 exon 3. In this analysis, the amplified PCR fragment was detected clearly in NB9 cells, but not in NB69 (Fig. 5D).

## Discussion

Many studies have shown that epigenetic alterations, especially aberrant DNA methylation, were involved in the development of various adult tumors (20,21). In neuroblastomas, aberrantly methylated genes, 64% for *THBS1*; 30% for *TIMP-3*; 27% for *MGMT*; 25% for *p73*; 18% for *RB1*; 14% for *DAPK*, *p14ARF*, *p16INK4a* and *CASP8*, respectively, and 0% for *TP53* and *GSTP1* have been reported and the striking differences in methylation status within neuroblastomas has suggested the existence of methylator phenotype, which might be associated with more aggressive forms of neuroblastoma (22,23). Neuroblastoma development is associated with aberration of neural differentiation, and we have reported that aberrant methylation in neuroblastoma at T-/DS-DMR, which plays an important role in differentiation and development (24).

Development of neuroblastoma is related with aberration of the function of neural development factors, such as NGF-dependent tyrosine kinase receptor TrkA activation, relating to differentiation in normal and neoplastic neuronal cells. NR4A are reported to play an important role in the development of neurons (25) and in the regulation of neural function (26). NR4A belongs to a group of early responsive genes, mediating fast response to pleiotropic extracellular stimuli. They bind to NGFI-B response element (NBRE), induce the downstream genes and affect many type of biological function such as oxidative metabolism, cell proliferation, differentiation, apoptosis and dopamine functions in the brain (9,27). In view of their role in brain function, it was reported that NR4A genes, including NR4A3, were induced by psychoactive drugs such as cocaine, morphine, haloperidol and clozapine (28). In cultured cerebellar granule neurons, NR4A transcripts translocated from nucleus to mitochondria during excitotoxicity, contributing to the induction of apoptosis (29).

Our present data about mouse brains also indicate the involvement of NR4A3 and its exon 3 CpGi methylation in the neural development. In the analysis of neuroblastoma specimens, NR4A3 exon 3 CpGi showed low methylation level in neuroblastoma compared with adrenal samples. In addition, hypermethylation of the *NR4A3* exon 3 CpGi was significantly associated with favorable outcome. Since there was a correlation between methylation level at *NR4A3* exon 3 CpGi and *NOR1* expression, our present data suggest that *NOR1* expression level and its genome methylation could be prognostic biomarkers in neuroblastoma.

Methylation of CpG sites at exonic region may be linked to epigenetic remodeling of genomic DNA structure. One of the factors is CCCTC binding factor (CTCF), which is highly conserved in higher eukaryotes. CTCF binds to CTCF-binding sites, and this binding is often regulated by DNA methylation. Of the CTCF-binding sites 45% are located on intergenic,

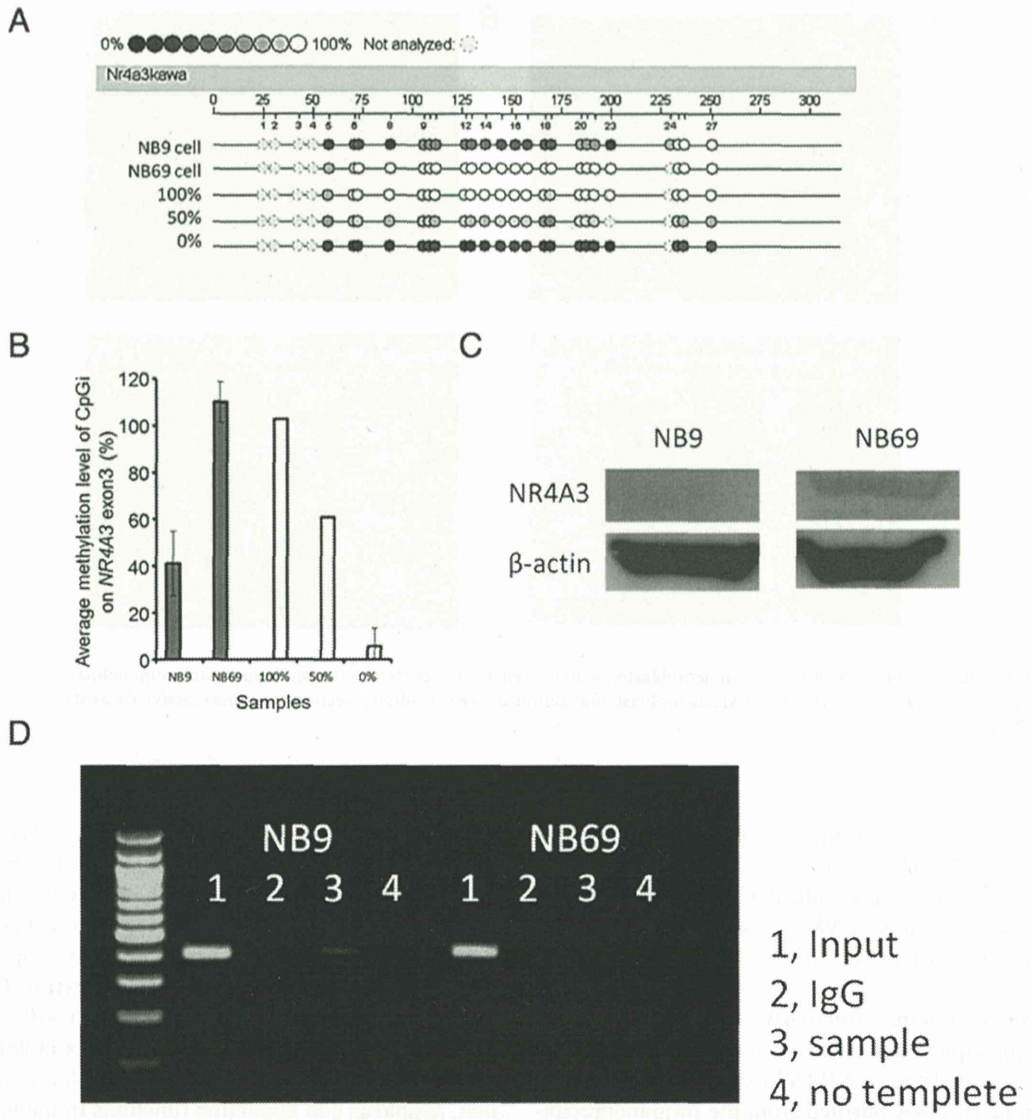


Figure 5. DNA methylation and protein expression levels of NR4A3 in human neuroblastoma cell lines. DNA methylation levels were analyzed quantitatively using Sequenom MassARRAY epiTYPER. (A) Methylation level of each CpG is shown in Epigram. (B) Average methylation level of each CpG site in this region is shown. Gray columns indicate neuroblastoma cell lines and open columns are the standard. Error bars indicate SD. (C) NR4A3 protein expression was analyzed by western blotting. NB69 showed high methylation level of the *NR4A3* gene and expressed NR4A3 protein, while hypomethylated NB9 cells did not express the protein. (D) Chromatin immunoprecipitation assay of NR4A3 exon 3 region. Crosslinked DNA-protein complexes were immunoprecipitated with anti-CTCF antibody and control antibodies, followed by PCR amplification using primers for NR4A3 exon 3. Precipitant from NB9 lysate contained NR4A3 exon 3 region, but no product was amplified in the precipitant from NB69 lysate.

7% 5'-untranslated region (UTR), 3% exonic, 29% intronic and 20% within 2.5 kb of promoters. H19 DMR is one of CTCF-binding sites and its methylation level is related to epigenetic remodeling, which is co-localized with cohesion. Aberrant regulation of CTCF expression is associated with occurrence of cancers, such as colorectal carcinoma (18,30,31). Our present study showed that CTCF can coimmunoprecipitate with a CTCF binding site within *NR4A3* exon 3 CpGi in NB9 cells but not in NB69 cells. This suggests hypermethylation of *NR4A3* exon 3 CpGi in NB69 cells may inhibit its binding to the CTCF and therefore initiate expression of NOR1. This expression regulation via CTCF binding may be a mechanism of NOR1 down-regulation and involved in advanced neuroblastomas and/or neuronal de-differentiation.

This is the first report indicating that DNA methylation level of *NR4A3* exon 3 CpGi is associated with NOR1 expression and aberrantly methylated in neuroblastomas. In addition, our present data suggest that hypermethylation of this region might be one of the prognostic factors in this tumor. Although further analyses are necessary to elucidate the regulation mechanism of NOR1 expression and its function, our present data strongly suggest that this gene could be involved in neural differentiation and human neuroblastomagenesis.

**Acknowledgements**

This study was supported by Nihon University Multidisciplinary Research Grant for 2006 (to H.N.), the Academic Frontier

Project for 2006 Project for Private Universities, a matching fund subsidy from MEXT (to H.N.), National Cancer Institute Grant CA102423 (to W.A.H and H.N.), National Cancer Institute Center Support Grant CA16056 (to Roswell Park Cancer Institute) and Grant-in-Aid from the Ministry of Education, Science, Sports and Culture of Japan (grant nos. 20592092 and 23300344).

## References

1. De Bernardi B, Nicolas B, Boni L, Indolfi P, Carli M, Cordero Di Montezemolo L, Donfrancesco A, Pession A, Provenzi M, di Cataldo A, Rizzo A, Tonini GP, Dallorso S, Conte M, Gambini C, Garaventa A, Bonetti F, Zanazzo A, D'Angelo P and Bruzzi P: Disseminated neuroblastoma in children older than one year at diagnosis: comparable results with three consecutive high-dose protocols adapted by the Italian Co-Operative Group for Neurobalstoma. J Clin Oncol 21: 1592-1601, 2003.
2. Matthay KK, Villablanca JG, Seeger RC, Stram DO, Harris RE, Ramsay NK, Swift P, Shimada H, Black CT, Brodeur GM, Gerbing RB and Reynolds CP: Treatment of high-risk neuroblsatoma with intensive chemotherapy, radiotherapy, autologous bone marrow transplantation, and 13-cis-retinoic acid. Children's Cancer Group. N Engl J Med 341: 1165-1173, 1999.
3. Wang H, Lee S, Nigro CL, Lattanzio L, Merlano M, Monteverde M, Matin R, Purdie K, Mladkova N, Bergamaschi D, Harwood C, Syed N, Szlosarek P, Briasoulis E, McHugh A, Thompson A, Evans A, Leigh I, Fleming C, Inman GJ, Hatzimichael E, Proby C and Crook T: NT5E (CD73) is epigenetically regulated in malignant melanoma and associated with metastatic site specificity. Br J Cancer 106: 1446-1452, 2012.
4. Geiman TM and Muegge K: DNA methylation in early development. Mol Reprod Dev 77: 105-113, 2010.
5. Bird A: DNA methylation patterns and epigenetic memory. Genes Dev 16: 6-21, 2002.
6. Weber M, Hellmann I, Stadler MB, Ramos L, Pääbo S, Rebhan M and Schübeler D: Distribution, silencing potential and evolutionary impact of promoter DNA methylation in the human genome. Nat Genet 39: 457-466, 2007.
7. Song F, Smith JF, Kimura MT, Morrow AD, Matsuyama T, Nagase H and Held WA: Association of tissue-specific differentially methylated regions (TDMs) with differential gene expression. Proc Natl Acad Sci USA 102: 3336-3341, 2005.
8. Eckhardt F, Lewin J, Cortese R, Rakyan VK, Attwood J, Burger M, Burton J, Cox TV, Davies R, Down TA, Haefliger C, Horton R, Howe K, Jackson DK, Kunde J, Koenig C, Liddle J, Niblett D, Otto T, Pettett R, Seemann S, Thompson C, West T, Rogers J, Olek A, Berlin K and Beck S: DNA methylation profiling of human chromosomes 6, 20 and 22. Nat Genet 38: 1378-1385, 2006.
9. Zhao Y and Bruemmer D: NR4A orphan nuclear receptors: transcriptional regulators of gene expression in metabolism and vascular biology. Arterioscler Thromb Vasc Biol 30: 1535-1541, 2010.
10. Maxwell MA and Muscat GE: The NR4A subgroup: immediate early response genes with pleiotropic physiological roles. Nucl Recept Signal 4: e002, 2006.
11. Song F, Mahmood S, Ghosh S, Liang P, Smiraglia DJ, Nagase H and Held WA: Tissue specific differentially methylated regions (TDMR): Changes in DNA methylation during development. Genomics 93: 130-139, 2009.
12. Li LC and Dahiya R: MethPrimer: designing primers for methylation PCRs. Bioinformatics 18: 1427-1431, 2002.
13. Ehrich M, Nelson MR, Stanssens P, Zabeau M, Liloglou T, Xinarianos G, Cantor CR, Field JK and van den Boom D: Quantitative high-throughput analysis of DNA methylation patterns by base-specific cleavage and mass spectrometry. Proc Natl Acad Sci USA 102: 15785-15790, 2005.
14. Fatemi M, Pao MM, Jeong S, Gal-Yam EN, Egger G, Weisenberger DJ and Jones PA: Footprinting of mammalian promoters: use of a CpG DNA mehtyltransferase revealing nucreosome positions at a single molecule level. Nucleic Acids Res 33: e176, 2005.
15. Baxter EW, Cummings WJ and Fournier REK: Formation of a large, complex domain of histone hyperacetylation at human 14q32.1 requires the serpin locus control region. Nucleic Acids Res 33: 3313-3322, 2005.
16. Orlando V, Strutt H and Paro R: Analysis of chromatin structure by in vivo formaldehyde cross-linking. Methods 11: 205-214, 1997.
17. Bowers SR, Mirabella F, Calero-Nieto FJ, Valeaux S, Hadjur S, Baxter EW, Merkenschlager M and Cockerill PN: A conserved insulator that recruits CTCF and cohesin exists between the closely related but divergently regulated interleukin-3 and granulocyte-macrophage colony-stimulating factor genes. Mol Cell Biol 29: 1682-1693, 2009.
18. Ishihara K, Oshimura M and Nakao M: CTCF-dependent chromatin insulator is linked to epigenetic remodeling. Mol Cell 23: 733-742, 2006.
19. Akoben AK: Understanding diagnostic tests 3: Receiver operating characteristic curves. Acta Paediatr 96: 644-647, 2007.
20. Egger G, Liang G, Aparicio A and Jones PA: Epigenetics in human disease and prospects for epigenetic therapy. Nature 27: 457-463, 2004.
21. Laird PW: Cancer epigenetics. Hum Mol Genet 15: 65-76, 2005.
22. Gonzalez-Gomez P, Bello MJ, Lomas J, Arjona D, Alonso ME, Amiñoso C, Lopez-Marin I, Anselmo NP, Sarasa JL, Gutierrez M, Casartelli C and Rey JA: Aberrant methylation of multiple genes in neuroblastic tumours. relationship with MYCN amplification and allelic status at 1p. Eur J Cancer 39: 1478-1485, 2003.
23. Banelli B, Vinci AD, Gelvi I, Casciano I, Allemanni G, Bonassi S and Romani M: DNA methylation in neuroblastic tumors. Cancer Lett 228: 37-41, 2005.
24. Kawashima H, Sugito K, Yoshizawa S, Uekusa S, Furuya T, Ikeda T, Koshinaga T, Shinojima Y, Hasegawa R, Mishra R, Igarashi J, Kimura M, Wang X, Fujiwara K, Gosh S and Nagase H: DNA hypomethylation at the ZNF206-exon 5 CpG island associated with neuronal differentiation in mice and development of neuroblastoma in humans. Int J Oncol 40: 31-39, 2012.
25. Zetterström RH, Williams R, Perlmann T and Olson L: Cellular expression of the immediate early transcription factors Nurr1 and NGFI-B suggests a gene regulatory role in several brain regions including the nigrostriatal dopamine system. Brain Res Mol Brain Res 5: 111-120, 1996.
26. Ohkura N, Ito M, Tsukada T, Sasaki K, Yamaguchi K and Miki K: Structure, mapping and expression of a human NOR-1 gene, the third member of the Nur77/NGFI-B family. Biochim Biophys Acta 1308: 205-214, 1996.
27. Eells JB, Wilcots J, Sisk S and Guo-Ross SX: NR4A gene expression is dynamically regulated in the ventral tegmental area dopamine neurons and is related to expression of dopamine neurotransmission genes. J Mol Neurosci 46: 545-553, 2012.
28. Werme M, Ringholm A, Olson L and Brené S: Differential patterns of induction of NGFI-B, Norl and c-fos mRNAs in striatal subregions by haloperidol and clozapine. Brain Res 863: 112-119, 2000.
29. Boldingh Debernard KA, Mathisen GH and Paulsen RE: Differences in NGFI-B, Nurr1, and NOR-1 expression and nucleocytoplasmic translocation in glutamate-treated neurons. Neurochem Int 61: 79-88, 2012.
30. Wendt KS, Yoshida K, Itoh T, Bando M, Koch B, Schirghuber E, Tsutsumi S, Nagae G, Ishihara K, Mishiro T, Yahata K, Imamoto F, Aburatani H, Nakao M, Imamoto N, Maeshima K, Shirahige K and Peters JM: Cohesin mediates transcriptional insulation by CCCTC-binding factor. Nature 451: 796-801, 2008.
31. Phillips JE and Corces VG: CTCF: master weaver of the genome. Cell 137: 1194-1211, 2009.

J Mol Med (2014) 92:509–521
DOI 10.1007/s00109-013-1118-x

JMolMed

ORIGINAL ARTICLE

# A novel gene regulator, pyrrole–imidazole polyamide targeting ABCA1 gene increases cholesterol efflux from macrophages and plasma HDL concentration

**Akiko Tsunemi · Takahiro Ueno · Noboru Fukuda · Takayoshi Watanabe · Kazunobu Tahira · Akira Haketa · Yoshinari Hatanaka · Sho Tanaka · Taro Matsumoto · Yoshiaki Matsumoto · Hiroki Nagase · Masayoshi Soma**

Received: 28 June 2013 / Revised: 29 November 2013 / Accepted: 16 December 2013 / Published online: 25 January 2014


**Abstract**
Pyrrole–imidazole (PI) polyamides are nuclease-resistant novel compounds that inhibit transcription factors by binding to the minor groove of DNA. A PI polyamide that targets mouse ABCA1 and increases ABCA1 gene expression was designed and evaluated as an agent to increase plasma HDL concentration. A PI polyamide was designed to bind the activator protein-2 binding site of the mouse ABCA1 promoter. The effect of this PI polyamide on ABCA1 expression was evaluated by real-time RT-PCR and Western blotting using RAW264 cells. In vivo effects of this polyamide on ABCA1 gene expression and plasma HDL level were examined in C57B6 mice. One milligram per kilogram of body weight of PI polyamide was injected via the tail veins every 2 days for 1 week, and plasma lipid profiles were evaluated. PI polyamide showed a specific binding to the target DNA in gel mobility shift assay. Treatment of RAW264 cells with 1.0 μM PI polyamide significantly increased ABCA1 mRNA expression. PI polyamide also significantly increased apolipoprotein AI-mediated HDL biogenesis in RAW264 cells. Cellular cholesterol efflux mediated by apolipoprotein AI was significantly increased by the PI polyamide treatment. PI polyamide significantly increased expression of ABCA1 mRNA in the liver of C57B6 mice. Plasma HDL concentration was increased by PI polyamide administration. All of the HDL sub-fractions showed a tendency to increase after PI polyamide administration. The designed PI polyamide that targeted ABCA1 successfully increased ABCA1 expression and HDL biogenesis. This novel gene-regulating agent is promising as a useful compound to increase plasma HDL concentration.

**Key messages**

- A novel pyrrole–imidazole (PI) polyamide binds to ABCA1.
- PI polyamide interfered with binding of AP-2 protein to the ABCA1 gene promoter.
- PI polyamide inhibited the AP-2 -mediated reduction of ABCA1 gene and protein expression.
- PI polyamide increased ABCA1 protein and apolipoprotein AI mediated HDL biogenesis.
- PI polyamide is a new gene regulator for the prevention of atherosclerotic diseases.

A. Tsunemi · T. Ueno (✉) · N. Fukuda · K. Tahira · A. Haketa · Y. Hatanaka · S. Tanaka · M. Soma
Department of Medicine, Division of Nephrology, Hypertension and Endocrinology, Nihon University School of Medicine, 30-1 Oyaguchi-kami, Itabashi, Tokyo, Japan
e-mail: ueno.takahiro@nihon-u.ac.jp

T. Ueno · M. Soma
Innovative Therapy Research Group, Nihon University Research Institute of Medical Science, Nihon University School of Medicine, 30-1 Oyaguchi-kami, Itabashi, Tokyo, Japan

T. Watanabe · H. Nagase
Chiba Cancer Center Research Institute, 666-2 Nitona, Chuo, Chiba, Japan

T. Matsumoto
Department of Functional Morphology, Division of Cell Regeneration and Transplantation, Nihon University School of Medicine, 30-1 Oyaguchi-kami, Itabasi, Tokyo, Japan

Y. Matsumoto
Department of Clinical Pharmacokinetics, College of Pharmacy, Nihon University, 7-7-1 Narashinodai, Funabashi, Chiba, Japan

M. Soma
Department of Medicine, Division of General Medicine, Nihon University School of Medicine, 30-1 Oyaguchi-kami, Itabashi, Tokyo, Japan

**Keywords** ABCA1 · PI polyamide · HDL · AP-2

## Introduction

Epidemiological evidence has confirmed the inverse relationship between high-density lipoprotein (HDL) cholesterol and coronary heart disease [1, 2]. Major clinical guidelines for the prevention and treatment of cardiovascular disease recognize HDL cholesterol as an independent risk factor [3–5]. The overloading of cholesterol in macrophages, regarded as foam cell formation, is one of the crucial steps in the early stage of atherosclerosis. Cholesterol molecules are not catabolized in mammalian somatic cells and must be transported to the liver for its degradation to bile acids. HDL is thought to play a central role in this pathway. The removal of excess cholesterol from macrophage foam cells by HDL and its principal apolipoprotein, apolipoprotein AI, is thought to be one of the key mechanisms underlying the atheroprotective properties of HDL [6, 7]. ATP binding cassette transporter A1 (ABCA1) plays a pivotal role in cholesterol efflux from macrophage foam cells [8]. Overexpression of ABCA1 in mice resulted in an increase of HDL and reduction of atherosclerosis [9, 10]. Accordingly, therapies that increase ABCA1 expression are a promising strategy for prevention and treatment of atherosclerosis. Expression of ABCA1 is highly regulated. Loading cholesterol into macrophages results in enhanced transcription of ABCA1 gene by a reaction mediated by oxysterol-activated liver X receptor (LXR) [11–13]. ABCA1 expression can also be increased by peroxisome proliferator-activated receptor (PPAR)$\alpha$ or PPAR$\gamma$ activators [14, 15]. Recently, Iwamoto et al. reported that activator protein (AP)2$\alpha$ negatively regulates the ABCA1 gene transcription to decrease HDL biogenesis [16, 17].

Pyrrole–imidazole polyamide (PI polyamide) compounds are a new class of synthetic DNA-binding ligands principally composed of *N*-methylpyrrole and *N*-methylimidazole amino acids. A binary code has been developed to correlate DNA-binding sequence specificity with antiparallel side-by-side ring pairings in the minor groove of DNA [18, 19]. A pairing of imidazole opposite pyrrole targets the G–C base pair, and pyrrole opposite imidazole targets the C–G base pair. Pyrrole–pyrrole degenerately targets T–A and A–T base pairs [20]. Initiation of transcription requires binding of transcription factors to the cognate DNA response elements in the gene promoter. PI polyamides do not require vectors or any other delivery devices to distribute into tissues or cells. They have superior cell and nuclear membrane permeability and bind the minor groove and block binding of transcription factors, inhibiting gene expression. PI polyamides may therefore be a new transcriptional gene regulating agents for the treatment of diseases [21–23].

In this study, we designed a PI polyamide targeting the ABCA1 promoter adjacent to the AP2 binding site to increase the ABCA1 gene expression; we then examined the effect of this polyamide on ABCA1 gene expression and plasma HDL levels.

## Methods

### Synthesis of PI polyamides

PI polyamide targeting ABCA1 was designed to span the boundary of the AP2 binding site of the ABCA1 promoter. PI polyamides were synthesized according to previously described methods [24, 25]. A mismatch polyamide was also designed and synthesized that did not bind to the transcription binding sites of ABCA1 promoter. The structural formula of PI polyamides used in this study are shown in Fig. 1.

### DNA binding assay

Fluorescein isothiocyanate (FITC)-labeled oligonucleotides including AP-2 binding sequence were synthesized for a gel mobility shift assay. Four picomoles of the FITC-labeled oligonucleotides was incubated with 4.0 pmol of PI polyamide for 1 h at 37 °C. The resulting complexes were separated by electrophoresis and visualized with the luminescent image analyzer LAS-3000 (Fujifilm, Tokyo, Japan).

### Chromatin immunoprecipitation (ChIP)

For in vitro experiments, RAW264 cells (Health Science Research Resource Bank, Han-nan, Japan) were cultured in RPMI1640 medium supplemented with 10 % fetal calf serum (FCS) (Invitrogen, Carlsbad, CA, USA) and 10 mg/dl streptomycin (Invitrogen).

Preparation and immunoprecipitation of chromatin was performed using a SimpleChIP Enzymatic Chromatin IP kit (Cell Signaling Technology) according to manufacturer's instructions and monoclonal anti-AP-2$\alpha$ antibody (Santa Cruz Biotechnology, Paso Robles, CA, USA). DNA samples were analyzed by 2 % agarose gel electrophoresis and real-time PCR using Fast SYBR Green Master Mix (Applied Biosystems, Foster City, CA, USA) and an ABI 7500 real-time PCR system (Applied Biosystems) according to the manufacturer's instructions. Cells were treated with 0, 0.1, or 1.0 μM PI polyamide targeting ABCA1 for 24 h before immunoprecipitation. Primers used in this assay were 5′-AACGAGCTTTTCCCCTTTCCT-3′ and 5′-TGCTAGCCTTCGGGAAACG-3′.

### Determination of mRNA expression

To determine the effect of PI polyamide on RAW264 ABCA1 mRNA expression, RAW264 were incubated with 1.0, 0.1, or 0.01 μM PI polyamide targeting ABCA1 or 1.0 μM mismatch